



Torney, C. J., Lloyd-Jones, D. J., Chevallier, M., Moyer, D. C., Maliti, H. T., Mwita, M., Kohi, E. M. and Hopcraft, J.G.C. (2019) A comparison of deep learning and citizen science techniques for counting wildlife in aerial survey images. *Methods in Ecology and Evolution*, 10(6), pp. 779-787.

There may be differences between this version and the published version. You are advised to consult the publisher's version if you wish to cite from it.

This is the peer reviewed version of the following article: Torney, C. J., Lloyd-Jones, D. J., Chevallier, M., Moyer, D. C., Maliti, H. T., Mwita, M., Kohi, E. M. and Hopcraft, J.G.C. (2019) A comparison of deep learning and citizen science techniques for counting wildlife in aerial survey images. *Methods in Ecology and Evolution*, 10(6), pp. 779-787, which has been published in final form at <http://dx.doi.org/10.1111/2041-210X.13165>

This article may be used for non-commercial purposes in accordance with [Wiley Terms and Conditions for Self-Archiving](#).

<http://eprints.gla.ac.uk/180086/>

Deposited on: 15 February 2019

A comparison of deep learning and citizen science techniques for counting wildlife in aerial survey images

Colin J. Torney^{a,*}, David J. Lloyd-Jones^{b,*}, Mark Chevallier^a, David C. Moyer^c, Honori T. Maliti^d, Machoke Mwita^d, Edward M. Kohi^d, J. Grant C. Hopcraft^e

^a*School of Mathematics and Statistics, University of Glasgow, Glasgow G12 8SQ, UK*

^b*FitzPatrick Institute of African Ornithology, DST-NRF Centre of Excellence, University of Cape Town, Rondebosch 7701, South Africa*

^c*Integrated Research Center, The Field Museum of Natural History, 1400 S. Lake Shore Drive, Chicago, United States of America*

^d*Tanzania Wildlife Research Institute, P.O.Box 661, Arusha, Tanzania*

^e*Institute of Biodiversity, Animal Health and Comparative Medicine, University of Glasgow, Glasgow G12 8QQ, UK*

Abstract

1. Fast and accurate estimates of wildlife abundance are an essential component of efforts to conserve ecosystems in the face of rapid environmental change. A widely used method for estimating species abundance involves flying aerial transects, taking photographs, counting animals within the images, then inferring total population size based on a statistical estimate of species density in the region. The intermediate task of manually counting the aerial images is highly labour intensive and is often the limiting step in making a population estimate.
2. Here we assess the use of two novel approaches to perform this task by deploying both citizen scientists and deep learning to count aerial images of the 2015 survey of wildebeest (*Connochaetes taurinus*) in Serengeti National Park, Tanzania.
3. Through the use of the online platform Zooniverse, we collected multiple non-expert counts by citizen scientists and used three different aggregation methods to obtain a single count for the survey images. We also counted the images by developing a bespoke deep learning method via the use of a convolutional neural network. The results of both approaches were then compared.
4. After filtering of the citizen science counts, both approaches provided highly accurate total estimates. The deep learning method was far faster and appears to be a more reliable and predictable approach, however we note that citizen science volunteers played an important role when creating training data for the algorithm. Notably, our results show that accurate, species-specific, automated counting of aerial wildlife images is now possible.

*authors contributed equally

28 **Second-language abstract**

29 1. Namna bora na ya haraka ya kuidadi wanyamapori ni jambo la msingi kwenye jitihada za uhifadhi na ikolojia
30 hasa wakati huu wa mabadiliko ya tabia nchi. Mojawapo ya njia ambayo hutumika kuidadi wanyamapori ni kupiga
31 picha za angani kwa kutumia ndege ndogo, kisha kuhesabu wanyamapori walioko kwenye picha hizo, na baadaye
32 kukokotoa idadi kutokana na ukubwa wa eneo husika. Kazi ambayo huwa ni inachukua muda mrefu ni kuhesabu
33 wanyamapori kwenye picha, ambayo hucheleweshwa ukokotoaji wa idadi ya wanyamapori.

34 2. Katika utafiti huu, tumetumia njia mbili za kuhesabu idadi ya wanyamapori kwenye picha anga zilizochukuliwa
35 mwaka 2015 katika Hifadhi ya Taifa ya Serengeti nchini Tanzania. Njia hizo ni kuhesabu kwa kutumia wataalam wa
36 kujitolea kwenye mtandao wa kijamii na nyingine ni kwa kutumia mfumo wa maalum wa kompyuta wa kung'amua
37 maumbo ya vitu.

38 3. Kwa kutumia mtandao wa kijamii wa "Zooniverse" tuliweza kufanya majumuisho ya idadi ya nyumbu walio-
39 hesabiwa na wataalamu mbalimbali wa kujitolea wa kijamii kutoka kwenye picha husika. Kwa upande mwingine,
40 tuliweza kuhesabu nyumbu wote kwenye picha husika kwa kutumia mfumo wa maalum wa kompyuta. Baadae, ma-
41 tokeo ya njia zote mbili yalilinganishwa.

42 4. Baada ya kulinganisha makossa ya wazi kwenye njia ya kuhesabu kwa kutumia ya watu wa kujitolea kwenye
43 mtandao wa kijamii, matokeo ya ukadiriaji wa idadi ya nyumbu kwa njia zote yalikuwa sawia. Hata hivyo, njia ya
44 mfumo wa kompyuta ilionesha kutoa matokeo kwa haraka na ya kuaminika. Aidha, tafiti inaonesha wataalamu wa
45 kujitolea wa kijamii ni wa muhimu katika kuandaa takwimu za kuufunza mfumo wa kompyuta uliotumika. Kwa
46 ujumla, matokeo ya utafiti wetu yameonesha uwezekano wa kuhesabu na kutambua nyumbu kwenye picha kwa kutu-
47 mia mfumo wa kompyuta.

48 **1. Introduction**

49 Estimating the abundance of animal species is essential for ecologists, conservationists, and wildlife managers
50 worldwide. Measuring population abundance enables the early detection of population declines (caused by disease,
51 over-harvesting, or changing patterns of land-use), or population increases and expansions; therefore it is a precursor
52 for adaptive management and conservation strategies (Walters, 1986). Repeated measurements of population abun-
53 dance also provide insight into the key factors that regulate natural populations (Turchin, 1999), a means to determine
54 their vital rates (Mduma et al., 1999), and are an essential requirement for validating theoretical models of species
55 interactions.

56 The challenge of detecting and responding to changes in animal abundance is especially acute in the case of
57 migratory species (Harris et al., 2009; Singh and Milner-Gulland, 2011). Estimating population sizes of migratory

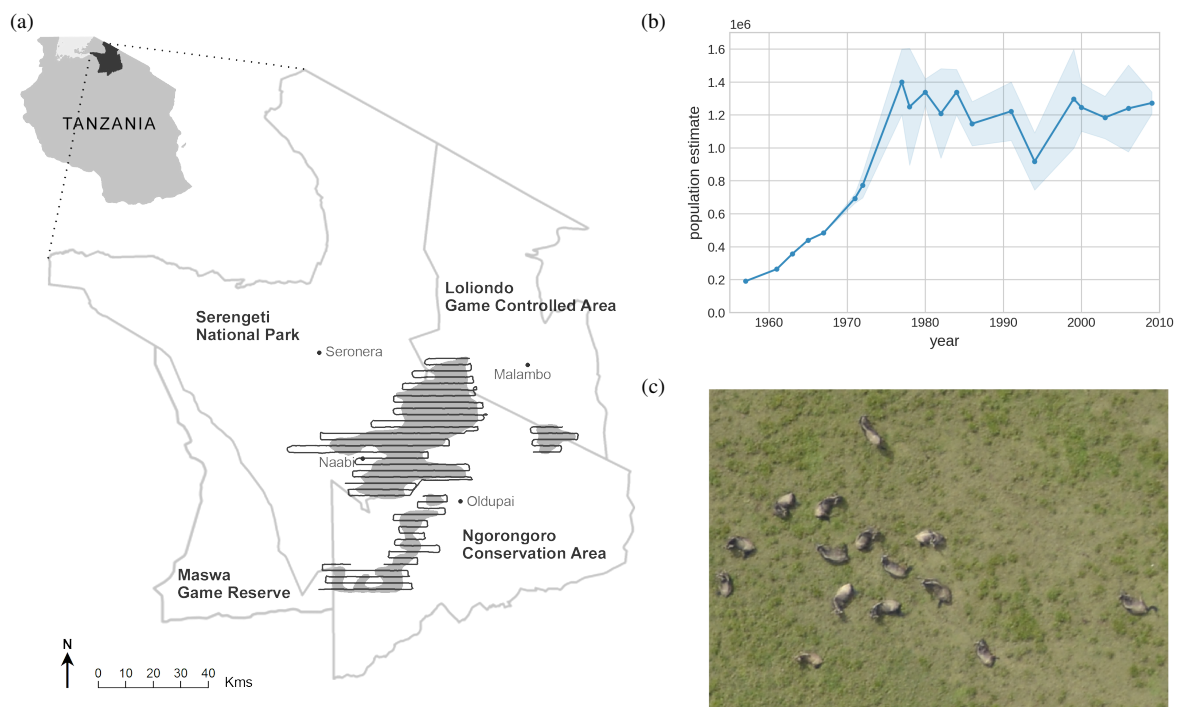


Figure 1: The Serengeti wildebeest census. (a) Map of the region showing the approximate distribution of the herds (shaded) and the transects flown during the 2015 census. (b) Wildebeest population estimates over time. Shaded region indicates the standard error of the estimate. Since the 1970s estimates have been made using the Jolly II method (Jolly, 1969) with data collected using vertical aerial photography and manual image counts. Images from a census conducted in 2018 are currently being manually processed. Infrequent counts with large errors highlight the need for new approaches. (c) An example section of a 2015 survey image showing a group of wildebeest.

58 species is a vital, but logistically challenging task. Localized environmental disturbances in large geographic areas are
59 often hard to detect, while the fact that migrations span national and regional borders, means implementing protection
60 strategies typically involves substantial time to coordinate (Lovejoy et al., 1987; Wilcove and Wikelski, 2008).

61 The Serengeti National Park in Tanzania is known for the iconic migration of approximately 1.3 million blue
62 wildebeest (*Connochaetes taurinus*) and 250,000 common zebra (*Equus quagga*). This is the largest terrestrial mi-
63 gration of animals on Earth (Thirgood et al., 2004) and their annual movement alters every biological process in
64 the ecosystem, from soil nutrient cycles, to the diversity of insects, birds and carnivores, to the balance of trees and
65 grass (Estes, 2014; Holdo et al., 2011b; McNaughton, 1985; Subalusky et al., 2017), as well as providing vital ecosys-
66 tem services to human communities around the park (Sinclair et al., 2015). Without the annual migratory cycle there
67 would be fundamental changes in the ecology of the region and much of its biodiversity would decline (Dobson et al.,
68 2010; Holdo et al., 2011a). The long-term population trend of the wildebeest (see Fig. 1) is closely tied to levels of
69 poaching, disease, climate change, and human perturbations. Therefore, estimating wildebeest abundance is perhaps
70 the most important metric of the ecosystem's health (Estes, 2014).

71 The standard approach to counting the wildebeest population is to fly transects over the herds in March, April
72 or May (Campbell and Borner, 1995; Norton-Griffiths, 1973) while the bulk of the wildebeest are on the short grass
73 plains in the south-east of Serengeti and the Ngorongoro conservation area, before the migration moves into the
74 woodland areas of the western Serengeti. As with many aggregated species, instead of performing in air counts, nadir
75 georeferenced aerial photographs are taken of the survey area at fixed intervals from an aircraft flown as close as
76 possible to a constant speed. The next stage of the process is then to identify and count all wildebeest within each
77 image. This process of manually counting each image is a labour-intensive process that typically takes three or four
78 skilled counters approximately 3-6 weeks (Torney et al., 2016). Automating this aspect of the survey would have
79 two major advantages. Firstly, it would remove a bottleneck in running the survey. Beyond the actual counting time,
80 there is often a considerable delay in scheduling the counting process as it involves multiple wildlife professionals
81 to undertake. Secondly, removing this time-consuming job would relieve a significant burden on the organizations
82 involved, freeing conservation professionals to focus on other tasks. Two novel methods can potentially replace
83 the use of manual counts by experts, the deployment of citizen scientists and the use of automated object detection
84 algorithms. In this work we deploy both approaches and evaluate the performance and merits of each.

85 1.1. Citizen science and the wisdom of crowds

86 It has long been noted that multiple non-expert individuals can be as accurate as a single expert for certain tasks if
87 their estimates are appropriately aggregated (Condorcet, 1976; Galton, 1907). This phenomenon represents collective
88 intelligence in its purest form, or as it's commonly known 'the wisdom of crowds' (Surowiecki, 2005) and in effect

89 means that as more individuals estimate some quantity of interest, then an appropriate aggregate quantity (Kao et al.,
90 2018) derived from these estimates will converge on the true value.

91 The wisdom of crowds is the basis for many attempts to harness the collective power of citizen scientists. The
92 key idea is that through online platforms, such as zooniverse (Simpson et al., 2014), scientists can outsource tasks
93 to non-experts and by aggregating multiple responses obtain usable, reliable data. Citizen science has been used in
94 multiple domains from protein folding (Dill and MacCallum, 2012) to astronomy (Lintott et al., 2008), and appears to
95 be growing as a tool for ecologists and conservationists (Ellwood et al., 2017; Swanson et al., 2016), where it has the
96 major advantage of not only performing scientific analysis of data but also engaging the public with wildlife conser-
97 vation (Forrester et al., 2017). However, despite the growth in the use and awareness of citizen science approaches,
98 there is still some skepticism about the reliability of unpaid and often anonymous volunteers (see (Kosmala et al.,
99 2016; Sauermann and Franzoni, 2015) for a review and discussion of these issues and potential mitigation strategies).

100 *1.2. Automated computer vision*

101 Another potential approach to replacing dedicated professional counters is to use machine learning algorithms.
102 Computer vision and machine learning are increasingly becoming essential components of the ecologist’s tool-
103 box (Bruijning et al., 2018; Christin et al., 2018; Dell et al., 2014; Mac Aodha et al., 2018; Valletta et al., 2017;
104 Weinstein, 2018) and have been applied previously to the task of counting aerial images of animals (Bajzak and Piatt,
105 1990; Chabot et al., 2018; Laliberte and Ripple, 2003; McNeill et al., 2011; Rey et al., 2017; Xue et al., 2017; Yang
106 et al., 2014) including the Serengeti wildebeest population (Torney et al., 2016).

107 While attempts to automate the classification and/or localisation of objects within images have been on-going
108 for decades, recently a combination of advances in machine learning, increased parallel computing power provided
109 by graphical processing units (GPUs), and accessibility of image training datasets, such as the COCO dataset (Lin
110 et al., 2014), have led to rapid improvements in the performance of multilayer deep convolutional neural networks
111 (DCNNs). These multilayer neural networks are a form of deep learning and are distinct to traditional machine
112 learning approaches to computer vision in that no hand-crafted features are required, instead the convolutional layers
113 extract relevant features directly from the training data. For image classification tasks, DCNNs achieved accuracy
114 levels that match the ability of humans a number of years ago (Szegedy et al., 2015). Computationally efficient object
115 detection is a more difficult task as it effectively involves multiple classifications of different regions within an image.
116 Recently, a number of specialized object detection networks have been developed that either use a two stage process
117 of proposing regions then classifying them (Girshick, 2015; Ren et al., 2015), or a single pass through the network
118 to predict object classes and their coordinates (Liu et al., 2016; Redmon et al., 2016; Redmon and Farhadi, 2017). In
119 this work we evaluate the performance of the single-pass DCNN architecture proposed in (Redmon et al., 2016) and

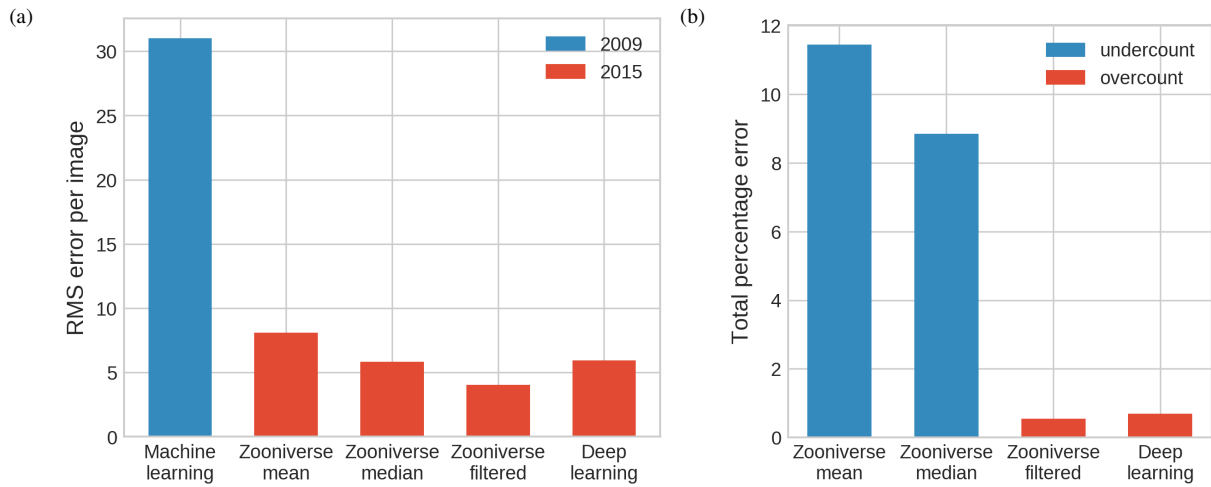


Figure 2: Error rates for the different methods calculated against the assumed true number of wildebeest per image as determined by the expert counter. (a) Root mean squared error calculated over 1000 test images counted using the different methods. For comparison we include results from (Torney et al., 2016), where handcrafted rotation invariant features were extracted and classified with a decision tree. It should be noted that the image resolution was lower in 2009 (4288x2848) and therefore a greater error should be expected. (b) The total percentage under or over count for 1000 survey images for the zooniverse data (aggregated using 3 different methods) and the deep learning algorithm.

120 iteratively refined in (Redmon and Farhadi, 2017, 2018), named YOLO which stands for *you only look once*, referring
 121 to the fact only a single pass through the network is required.

122 2. Methods

123 2.1. Aerial surveys

124 The 2015 Serengeti wildebeest count was conducted between the 23rd April and 2nd May over the eastern and
 125 southern plains of Serengeti National Park, Ngorongoro Conservation Area, Loliondo Game Controlled Area, and
 126 Maswa Game Reserve. A Cessna C182 aircraft was used to conduct the survey, with photographs taken using a
 127 NIKON D800 through a 35mm Nikor Lens. The camera was mounted in a port in the floor of the aircraft and images
 128 were manually triggered at the start of each transect to be collected automatically every 10 seconds.

129 Reconnaissance flights over several days prior to the count identified the distribution of the migratory herd and
 130 from these flights the herd distribution was mapped, and a survey frame identified. When the distribution was optimal,
 131 10.3 hours of photographic sampling flights were flown along east-west transects on 30 April and 2 May covering a
 132 straight-line distance of 2040 km.

133 During the count, flight target altitude along transects was 700ft (213m) above the ground. This was an optimal
 134 height to both maximise image resolution but not startle the wildebeest into running from the sound of the aircraft
 135 engine. Ground speed was maintained as closely as possible to 100 knots (185 km/h). A total of 1584 georeferenced
 136 images were taken with a resolution of 7360x4912 pixels.

137 *2.2. Zooniverse image counts*

138 The citizen science approach was facilitated by development of a wildebeest counting website using the zooniverse
139 platform (Simpson et al., 2014). Images were first filtered to remove those that were known to definitely not contain
140 any wildebeest. This step was taken to reduce the number of images that needed to be uploaded and, more importantly,
141 reduce the number of empty images that citizen counters needed to process.

142 Following initial trials on the website in August 2015 it was determined that volunteers would struggle to count
143 entire aerial images due to their large size and high resolution. Our solution was to split each aerial image into 12
144 equal-sized tiles. The images were uploaded to the Serengeti Wildebeest Count project on the zooniverse platform,
145 which included an information page, a *Field Guide* to help with the identification of wildebeest and other animals,
146 and the actual display of images where users could click on the images to indicate where they thought a wildebeest
147 was present. The pixel locations of each click were then recorded.

148 A total of 9,870 images were counted by 2,212 volunteers between the 10th of May and 31st of May 2017. Anyone
149 could visit the website and count wildebeest, and each image was counted by 15 different volunteers. Once an image
150 was counted 15 times it was retired and the overall project progress was displayed on a statistics bar on the home page.
151 Once all images were retired the classification data was downloaded. The data included the number of wildebeest
152 counted by each user, their username (unregistered users were given a random username) and the pixel location of
153 each of their identifications. Prior to analysis, any count data made using early versions of the counting interface or
154 collected by either developers or citizen scientists during testing of the interface functionality was removed.

155 *2.3. Implementation of object detection algorithm*

156 To automate the image counts we implemented the YOLOv3 (Redmon and Farhadi, 2018) object detector us-
157 ing the open source deep learning packages Keras (Chollet et al., 2015) and TensorFlow (Abadi et al., 2016). The
158 implementation of the algorithm followed three main steps.

159 Firstly, we generated a training dataset by selecting 500 of the survey images at random to be used exclusively for
160 training. Images were tiled into 864x864 sub-images and then passed through a version of the YOLO DCNN using
161 pre-trained weights from the COCO dataset provided by (Redmon and Farhadi, 2018). This process created a list of
162 the locations of potential objects in each image. As a first pass these results were filtered by discarding any object
163 detections that did not correspond to an identification from the zooniverse data. After this initial filter, the bounding
164 boxes were manually checked and corrected for each of the 20,000 training images (500 full size images were each
165 divided into 40 864x864 training images).

166 With this training set, we next made several minor modifications to the YOLOv3 architecture. YOLOv3 employs
167 9 predefined object shapes, termed anchor boxes, as initial estimates for object bounding box heights and widths. As

168 there was less variation in our target objects, we reduced the number of anchor boxes used from 9 to 3, and replaced
169 the dimensions of the 3 anchor boxes to match the training dataset. We next removed all but the final scale boxes
170 (YOLOv3 is a multiscale detector whereas for our application objects are only present at a single scale). Finally, we
171 modified the training loss function to suppress false positives and account for the large amounts of empty space in the
172 training images. We achieved this by increasing the weighting (from 0.5 to 2) given to the no-object component of
173 the multipart loss function described in Redmon et al. (2016). For training we used transfer learning, again using the
174 pre-trained general purpose YOLO object detector as a starting point with initial weights created by training on the
175 COCO dataset (Redmon and Farhadi, 2018). During training we first froze all but the final 7 layers of the network
176 and trained for 25 epochs, using the Adam optimiser and a learning rate of 10^{-4} . We then unfroze all layers, reduced
177 the learning rate to 10^{-6} , and trained for a further 20 epochs. In total training took 34 hours on a NVIDIA Quadro
178 GP100 GPU. Other parameters of the algorithm, the detection threshold and bounding box overlap (non-maximum
179 suppression) threshold, were selected based on minimising the difference between the automated count of the training
180 images and the expert count. All code is available from <https://github.com/ctorney/deepWildCount>

181 For the final stage we counted 1000 survey images selected at random, but excluding the 500 training images.
182 Counting the test images took 2 hours using the same GPU as for the training.

183 *2.4. Expert count*

184 The full set of images was counted, from January 28 to February 29 2018, by a single expert counter (DJL) using
185 Adobe CS6 as a viewing program operating on a Windows 10 operating system. Each JPEG was initially open in 'Fit'
186 mode before enlarging to 50% or greater and counted using a left to right, top to bottom scanning pattern. Counting
187 was conducted by clicking on and marking each wildebeest. The number of animals in each image were counted
188 twice — first as running tally during marking and secondly as a recount of the marks within the image. While there
189 remains the potential for bias in the expert count, we take this count to be the gold standard. Hence our results are
190 a comparison between the two novel methods employed and a count by a single experienced expert, which could in
191 principle deviate from the unknown true count.

192 **3. Results**

193 We compared the accuracy of the methods by calculating the deviation of each method from the single expert
194 count which we assume to be the true number of wildebeest in each image. For both the citizen science count and the
195 YOLO count we assess the accuracy across 1000 sample survey images. For the citizen science data this means that
196 empty images that were not uploaded to zooniverse are included when assessing accuracy. In effect by comparing

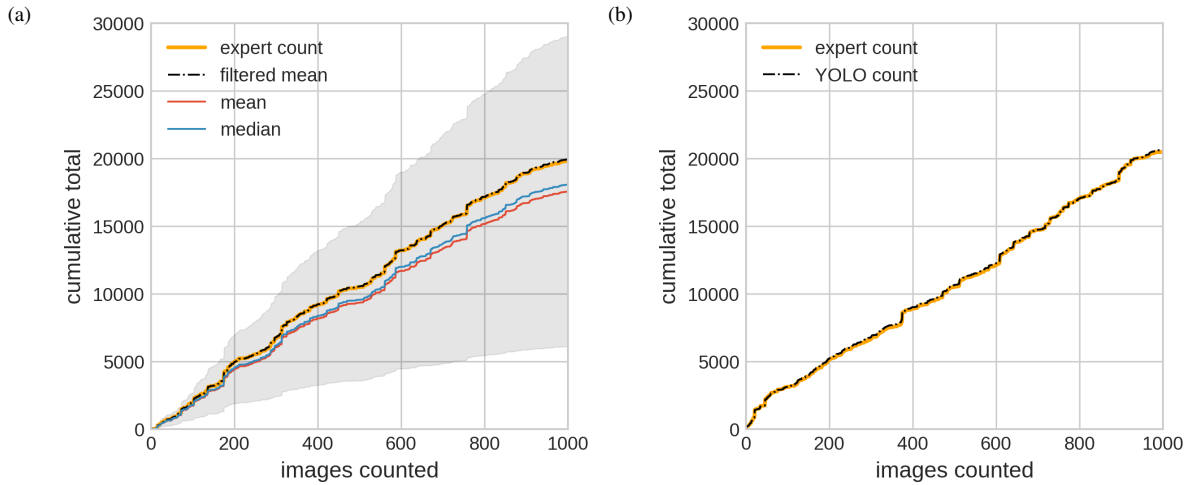


Figure 3: Cumulative image counts. (a) Mean, median and filtered mean for the zooniverse count data compared to the expert count. The shaded region indicates the cumulative count that would be recorded if the highest or lowest counts for each tile of each image were used. (b) The YOLO count compared with the expert count.

197 the methods in this way we are assuming that completely empty images will be processed by citizen scientists with
 198 perfect accuracy.

199 To aggregate the zooniverse data we adopted three approaches. We took the mean of the 15 counts, the median of
 200 the 15 counts, or removed the 5 lowest counts for each tile and took the mean of the remaining 10. For the last metric,
 201 the filtered mean, we determined which outliers to remove by minimizing the root mean squared (RMS) error on the
 202 test dataset, i.e. we removed 5 outliers in total but taking different numbers of highest or lowest counts, compared each
 203 combination to the expert counts and found that the optimal filtering was to remove the 5 lowest counts. We stress
 204 that the optimal filtering was determined on the same images used to assess the method hence there is no division of
 205 train and test images.

206 The per image error rates and total counts from the 1000 images are shown in Table 1 and Figure 2. From these
 207 results we see that all methods result in low per image error rate. However, while the average zooniverse counts and
 208 the deep learning algorithm have similar RMS errors, there is a clear discrepancy when examining the total counts
 209 summed over all 1000 images. The zooniverse volunteers showed a systematic tendency to undercount the images,
 210 hence there was approximately an 11% and 9% undercount for the total dataset for both the mean and the median. The
 211 YOLO algorithm did not show any systematic bias and although on average miscounted 1.7 wildebeest per image,
 212 its total was highly accurate, recording 20,631 wildebeest when the expert counted 20,489. Only the filtered mean,
 213 which averaged over the highest 10 volunteer counts, is comparable to the YOLO count in this respect.

214 We countered the systematic bias observed in the zooniverse data by filtering the lowest 5 estimates and taking
 215 the mean of the remaining 10 to obtain a highly accurate count. In Fig. 3 we show the cumulative counts across the

Method	Mean abs. error	RMS error	Percent overcount
Mean zooniverse	2.8	8.11	-11.44%
Median zooniverse	1.83	5.85	-8.85%
Filtered zooniverse	1.58	4.05	0.55%
YOLO	1.70	5.94	0.69%

Table 1: Summary of key comparison statistics. Error rates are calculated across 1000 survey images containing 19,802 wildebeest (zooniverse) and 20,489 wildebeest (YOLO).

216 1000 images for the aggregated zooniverse data and the highest and lowest counts for each image. From this figure
217 it is clear that the expert count is not at the centre of the distribution of zooniverse counters. Instead a more accurate
218 estimate is obtained by taking the mean of the 10 highest counts. It should be noted that both the mean and the median
219 display this systematic bias, therefore it is not simply due to the mean being a less robust estimator (Galton, 1907) but
220 instead reveals a tendency for all zooniverse counters, on average, to undercount. Whether this bias is persistent or
221 predictable can only be revealed by repeated citizen science counts of the survey and comparison to expert counts.

222 4. Discussion

223 From our results we see that both citizen science and deep learning methods are capable of producing highly
224 accurate image counts. Counting the wildebeest within the survey images is a difficult and time-consuming task.
225 When collecting the census images there are multiple trade-offs between aircraft height, flight speed, and camera
226 parameters (ISO, exposure etc.) that have to be balanced, with the result that image quality is often inconsistent.
227 While wildebeest are often clear and unambiguous (see Fig 1c), in many cases a subjective judgment has to be made
228 based on the balance of probabilities, i.e. what other animals are in the vicinity, or what landscape features are present.
229 In this context we should not expect perfect agreement between our methods but estimates within 1% of the total can
230 be considered as highly accurate.

231 For the citizen science counts we observe a systematic bias in the errors the counters made. These results sug-
232 gest that for a volunteer scientist the probability to miss a wildebeest is greater than the probability of incorrectly
233 identifying another object or animal as a wildebeest. This is in line with prior expectations; given some guidance on
234 identifying wildebeest (as was available on the zooniverse project page), false positives should be minimal. However
235 eliminating false negatives requires substantial focus, and it's likely that concentration will wane over time, or volun-
236 teers will become distracted. Highly populated images have to be meticulously annotated while, equally, seemingly
237 empty images have to be carefully scanned.

238 We found that it was possible to correct for this bias by removing the lowest 5 estimates. While this gives highly
239 accurate total counts and low per image error rates, there is no guarantee that the approach is transferable and how to

240 appropriately filter the data may be affected by the wording of the guidelines, the image resolution and sizes used, or
241 the set of volunteers that participate in the project. Other more sophisticated approaches to processing citizen science
242 data have been proposed (Swanson et al., 2016), however given the range of counts provided by the volunteers and
243 the large errors we observe in the baseline metrics ($\sim 11\%$ and $\sim 9\%$ undercount for the mean and median respectively)
244 there will need to be a rigorous process of validation before a citizen science count could be used as the sole basis for
245 a population estimate. Note, that if we simply took the minimum or maximum count per image the total count could
246 have been either half or almost double the true count. While suppression of these types of outliers is fundamentally
247 part of the ethos of citizen science, this does illustrate the broad range of responses from volunteers.

248 Considering the deep learning algorithm, we find that with minor modification and bespoke training, the object
249 detection network proposed by Redmon and Farhadi (2018) is able to rapidly count 1000 images and come up with a
250 total that is within 1% of an expert count. As other authors have shown, DCNNs are able to process wildlife images
251 for classification tasks (Chen et al., 2014; Norouzzadeh et al., 2018; Villa et al., 2017) and also detect and localise
252 animals (Maire et al., 2015; Schneider et al., 2018). YOLO has the advantage of being a single-pass object detector
253 that is fast and accurate. The 1000 images can be processed in under 2 hours, meaning every future census could be
254 counted within 24 hours. Hence a process that currently takes 3 to 6 weeks, involving 3-4 wildlife professionals and
255 countless cups of tea, can potentially be replaced with an automated system that runs overnight.

256 Image classification using pretrained DCNNs with state-of-the-art architectures (He et al., 2016; Simonyan and
257 Zisserman, 2014) can be achieved with a few lines of code using open source libraries such as Keras (Chollet et al.,
258 2015), while object detection algorithms are increasingly being integrated into libraries such as TensorFlow (Abadi
259 et al., 2016). Currently the greatest challenge for implementing these algorithms for bespoke applications is obtaining
260 sufficiently large training datasets. In this regard citizen scientists have a clear role to play. While we have shown that
261 the trained algorithm achieves high accuracy levels, it should be noted that the algorithm employed the crowd-sourced
262 data to create the training sets. Hence, both methods should be viewed as complementary approaches with citizen
263 science data forming the foundation for automated algorithms (Rey et al., 2017).

264 Our results show that deep learning algorithms are now at a state where they can legitimately replace manual
265 counters and remove a large burden from conservation organisations. The further great advantage of automated
266 image processing is that it will allow us to leverage emerging image collection technologies, such as unmanned aerial
267 vehicles, satellite platforms, or fixed camera traps; coupling these advances in image collection tools with automated
268 processing will greatly increase the accuracy of population estimates. As we move towards fully automated wildlife
269 counts, it only remains to ensure the availability of sufficient training data that is representative of all potential survey
270 images. This can be achieved by combining state-of-the-art deep learning methods with validated crowd-sourced

271 training data.

272 An automated wildebeest image count will not only be a significant benefit for monitoring this specific population
273 but provides a transferable methodology that can be deployed for any population monitoring that currently includes
274 manual image counts.

275 **Author contributions** CJT, JCGH, DJLJ designed the study. DJLJ, DCM, HTM, MM, EMK, JGCH collected data. CJT, DJLJ, MC, JGCH
276 analysed the data. CJT wrote the manuscript with input from all authors.

277 **Acknowledgements** JGCH acknowledges support from the British Ecological Society large grant scheme, the Friedkin Foundation, and the Eu-
278 ropean Union Horizon 2020 grant No 641918. CJT acknowledges support from a James S. McDonnell Foundation Studying Complex Systems
279 Scholar Award. We thank Anthony Dell for comments that improved the manuscript, we gratefully acknowledge the effort of the zooniverse vol-
280 unteers who counted wildebeest, and thank Alexandra Swanson for assistance with data extraction code and comments on the manuscript. This
281 publication uses data generated via the Zooniverse.org platform, development of which is funded by generous support, including a Global Impact
282 Award from Google, and by a grant from the Alfred P. Sloan Foundation.

283 **Data Accessibility** Raw count data are available from Enlighten: Research Data (<http://dx.doi.org/10.5525/gla.researchdata.732>).
284 Source code is available from <http://dx.doi.org/10.5281/zenodo.2562058>.

285 Abadi, M., Barham, P., Chen, J., Chen, Z., Davis, A., Dean, J., Devin, M., Ghemawat, S., Irving, G., Isard, M., et al., 2016. Tensorflow: A system
286 for large-scale machine learning. In: OSDI. Vol. 16. pp. 265–283.

287 Bajzak, D., Piatt, J. F., 1990. Computer-aided procedure for counting waterfowl on aerial photographs. *Wildlife Society Bulletin*, 125–129.

288 Bruijning, M., Visser, M. D., Hallmann, C. A., Jongejans, E., 2018. trackdem: Automated particle tracking to obtain population counts and size
289 distributions from videos in r. *Methods in Ecology and Evolution* 9 (4), 965–973.

290 Campbell, K., Borner, M., 1995. Population trends and distribution of serengeti herbivores: implications for management. *Serengeti II: Dynamics,*
291 *management, and conservation of an ecosystem*, 117–145.

292 Chabot, D., Dillon, C., Francis, C., 2018. An approach for using off-the-shelf object-based image analysis software to detect and count birds in
293 large volumes of aerial imagery. *Avian Conservation and Ecology* 13 (1).

294 Chen, G., Han, T. X., He, Z., Kays, R., Forrester, T., 2014. Deep convolutional neural network based species recognition for wild animal monitoring.
295 In: *Image Processing (ICIP), 2014 IEEE International Conference on*. IEEE, pp. 858–862.

296 Chollet, F., et al., 2015. Keras.

297 Christin, S., Hervet, E., Lecomte, N., 2018. Applications for deep learning in ecology. *bioRxiv*, 334854.

298 Condorcet, M., 1976. Essay on the application of mathematics to the theory of decision-making. Reprinted in *Condorcet: Selected Writings*, Keith
299 Michael Baker, ed 33.

300 Dell, A. I., Bender, J. A., Branson, K., Couzin, I. D., de Polavieja, G. G., Noldus, L. P., Pérez-Escudero, A., Perona, P., Straw, A. D., Wikelski, M.,
301 et al., 2014. Automated image-based tracking and its application in ecology. *Trends in ecology & evolution* 29 (7), 417–428.

302 Dill, K. A., MacCallum, J. L., 2012. The protein-folding problem, 50 years on. *Science* 338 (6110), 1042–1046.

303 Dobson, A. P., Borner, M., Sinclair, A. R. E., Hudson, P. J., Anderson, T. M., Bigurube, G., Davenport, T. B. B., Deutsch, J., Durant, S. M., Estes,
304 R. D., Estes, A. B., Fryxell, J., Foley, C., Gadd, M. E., Haydon, D., Holdo, R., Holt, R. D., Hopcraft, J. G. C., Hilborn, R., Jambiya, G. L. K.,
305 Laurenson, M. K., Melamari, L., Morindat, A. O., Ogotu, J. O., Schaller, G., Wolanski, E., 16 Sep. 2010. Road will ruin serengeti. *Nature*
306 467 (7313), 272–273.

307 Ellwood, E. R., Crimmins, T. M., Miller-Rushing, A. J., 2017. Citizen science and conservation: recommendations for a rapidly moving field.
308 Estes, R., 12 Apr. 2014. *The Gnu's World: Serengeti Wildebeest Ecology and Life History*. Univ of California Press.

309 Forrester, T. D., Baker, M., Costello, R., Kays, R., Parsons, A. W., McShea, W. J., 2017. Creating advocates for mammal conservation through
310 citizen science. *Biological Conservation* 208, 98–105.

311 Galton, F., 1907. Vox populi (the wisdom of crowds). *Nature* 75 (7), 450–451.

312 Girshick, R., 2015. Fast r-cnn. In: *Computer Vision (ICCV), 2015 IEEE International Conference on*. IEEE, pp. 1440–1448.

313 Harris, G., Thirgood, S., Hopcraft, J. G. C., Cromsigt, J. P., Berger, J., 2009. Global decline in aggregated migrations of large terrestrial mammals.
314 *Endangered Species Research* 7 (1), 55–76.

315 He, K., Zhang, X., Ren, S., Sun, J., 2016. Deep residual learning for image recognition. In: *Proceedings of the IEEE conference on computer vision*
316 *and pattern recognition*. pp. 770–778.

317 Holdo, R. M., Fryxell, J. M., Sinclair, A. R. E., Dobson, A., Holt, R. D., 25 Jan. 2011a. Predicted impact of barriers to migration on the serengeti
318 wildebeest population. *PLoS One* 6 (1), e16370.

319 Holdo, R. M., Holt, R. D., Sinclair, A. R. E., Godley, B. J., Thirgood, S., 2011b. Migration impacts on communities and ecosystems: empirical
320 evidence and theoretical insights. In: *Animal Migration*. pp. 130–143.

321 Jolly, G., 1969. Sampling methods for aerial censuses of wildlife populations. *East African Agricultural and Forestry Journal* 34 (sup1), 46–49.

322 Kao, A. B., Berdahl, A. M., Hartnett, A. T., Lutz, M. J., Bak-Coleman, J. B., Ioannou, C. C., Giam, X., Couzin, I. D., 2018. Counteracting
323 estimation bias and social influence to improve the wisdom of crowds. *Journal of The Royal Society Interface* 15 (141), 20180130.

324 Kosmala, M., Wiggins, A., Swanson, A., Simmons, B., 2016. Assessing data quality in citizen science. *Frontiers in Ecology and the Environment*
325 14 (10), 551–560.

326 Laliberte, A. S., Ripple, W. J., 2003. Automated wildlife counts from remotely sensed imagery. *Wildlife Society Bulletin*, 362–371.

- 327 Lin, T.-Y., Maire, M., Belongie, S., Hays, J., Perona, P., Ramanan, D., Dollár, P., Zitnick, C. L., 2014. Microsoft coco: Common objects in context.
328 In: European conference on computer vision. Springer, pp. 740–755.
- 329 Lintott, C. J., Schawinski, K., Slosar, A., Land, K., Bamford, S., Thomas, D., Raddick, M. J., Nichol, R. C., Szalay, A., Andreescu, D., et al.,
330 2008. Galaxy zoo: morphologies derived from visual inspection of galaxies from the sloan digital sky survey. *Monthly Notices of the Royal*
331 *Astronomical Society* 389 (3), 1179–1189.
- 332 Liu, W., Anguelov, D., Erhan, D., Szegedy, C., Reed, S., Fu, C.-Y., Berg, A. C., 2016. Ssd: Single shot multibox detector. In: European conference
333 on computer vision. Springer, pp. 21–37.
- 334 Lovejoy, T. E., Sallaberry, M., Senner, S. E., Tarak, A., 1987. Conservation strategy for migratory species. *American Scientist* 75, 19–26.
- 335 Mac Aodha, O., Gibb, R., Barlow, K. E., Browning, E., Firman, M., Freeman, R., Harder, B., Kinsey, L., Mead, G. R., Newson, S. E., et al., 2018.
336 Bat detective—deep learning tools for bat acoustic signal detection. *PLoS computational biology* 14 (3), e1005995.
- 337 Maire, F., Alvarez, L. M., Hodgson, A., 2015. Automating migratory mammal detection in aerial images captured during wildlife surveys: a deep
338 learning approach. In: Australasian Joint Conference on Artificial Intelligence. Springer, pp. 379–385.
- 339 McNaughton, S. J., 1985. Ecology of a grazing ecosystem: The serengeti. *Ecol. Monogr.* 55 (3), 259–294.
- 340 McNeill, S., Barton, K., Lyver, P., Pairman, D., 2011. Semi-automated penguin counting from digital aerial photographs. In: Geoscience and
341 Remote Sensing Symposium (IGARSS), 2011 IEEE International. IEEE, pp. 4312–4315.
- 342 Mduma, S. A., Sinclair, A., Hilborn, R., 1999. Food regulates the serengeti wildebeest: A 40-year record. *Journal of Animal Ecology* 68 (6),
343 1101–1122.
- 344 Norouzzadeh, M. S., Nguyen, A., Kosmala, M., Swanson, A., Palmer, M. S., Packer, C., Clune, J., 2018. Automatically identifying, counting, and
345 describing wild animals in camera-trap images with deep learning. *Proceedings of the National Academy of Sciences*, 201719367.
- 346 Norton-Griffiths, M., 1973. Counting the serengeti migratory wildebeest using two-stage sampling. *African Journal of Ecology* 11 (2), 135–149.
- 347 Redmon, J., Divvala, S., Girshick, R., Farhadi, A., 2016. You only look once: Unified, real-time object detection. In: Proceedings of the IEEE
348 conference on computer vision and pattern recognition. pp. 779–788.
- 349 Redmon, J., Farhadi, A., 2017. Yolo9000: better, faster, stronger. arXiv preprint.
- 350 Redmon, J., Farhadi, A., 2018. YoloV3: An incremental improvement. arXiv preprint arXiv:1804.02767.
- 351 Ren, S., He, K., Girshick, R., Sun, J., 2015. Faster r-cnn: Towards real-time object detection with region proposal networks. In: Advances in neural
352 information processing systems. pp. 91–99.
- 353 Rey, N., Volpi, M., Joost, S., Tuia, D., 2017. Detecting animals in african savanna with uavs and the crowds. *Remote Sensing of Environment* 200,
354 341–351.
- 355 Saueremann, H., Franzoni, C., 2015. Crowd science user contribution patterns and their implications. *Proceedings of the National Academy of*
356 *Sciences* 112 (3), 679–684.
- 357 Schneider, S., Taylor, G. W., Kremer, S. C., 2018. Deep learning object detection methods for ecological camera trap data. arXiv preprint
358 arXiv:1803.10842.
- 359 Simonyan, K., Zisserman, A., 2014. Very deep convolutional networks for large-scale image recognition. arXiv preprint arXiv:1409.1556.
- 360 Simpson, R., Page, K. R., De Roure, D., 2014. Zooniverse: observing the world's largest citizen science platform. In: Proceedings of the 23rd
361 international conference on world wide web. ACM, pp. 1049–1054.
- 362 Sinclair, A. R. E., Metzger, K. L., Mduma, S. A. R., Fryxell, J. M., 11 May 2015. Serengeti IV: Sustaining Biodiversity in a Coupled Human-Natural
363 System. University of Chicago Press.
- 364 Singh, N. J., Milner-Gulland, E. J., 2011. Conserving a moving target: planning protection for a migratory species as its distribution changes.
365 *Journal of Applied Ecology* 48 (1), 35–46.
- 366 Subalusky, A. L., Dutton, C. L., Rosi, E. J., Post, D. M., 19 Jun. 2017. Annual mass drownings of the serengeti wildebeest migration influence
367 nutrient cycling and storage in the mara river. *Proc. Natl. Acad. Sci. U. S. A.*
- 368 Surowiecki, J., 2005. The wisdom of crowds. Anchor.
- 369 Swanson, A., Kosmala, M., Lintott, C., Packer, C., 2016. A generalized approach for producing, quantifying, and validating citizen science data
370 from wildlife images. *Conservation Biology* 30 (3), 520–531.
- 371 Szegedy, C., Liu, W., Jia, Y., Sermanet, P., Reed, S., Anguelov, D., Erhan, D., Vanhoucke, V., Rabinovich, A., 2015. Going deeper with convolutions.
372 In: Proceedings of the IEEE conference on computer vision and pattern recognition. pp. 1–9.
- 373 Thirgood, S., Mosser, A., Tham, S., Hopcraft, G., Mwangomo, E., Mlengya, T., Kilewo, M., Fryxell, J., Sinclair, A. R. E., Borner, M., 2004. Can
374 parks protect migratory ungulates? the case of the serengeti wildebeest. *Anim. Conserv.* 7 (2), 113–120.
- 375 Torney, C. J., Dobson, A. P., Borner, F., Lloyd-Jones, D. J., Moyer, D., Maliti, H. T., Mwitia, M., Fredrick, H., Borner, M., Hopcraft, J. G. C., 2016.
376 Assessing rotation-invariant feature classification for automated wildebeest population counts. *PLoS one* 11 (5), e0156342.
- 377 Turchin, P., 1999. Population regulation: a synthetic view. *Oikos*, 153–159.
- 378 Valletta, J. J., Torney, C., Kings, M., Thornton, A., Madden, J., 2017. Applications of machine learning in animal behaviour studies. *Animal*
379 *Behaviour* 124, 203–220.
- 380 Villa, A. G., Salazar, A., Vargas, F., 2017. Towards automatic wild animal monitoring: Identification of animal species in camera-trap images using
381 very deep convolutional neural networks. *Ecological informatics* 41, 24–32.
- 382 Walters, C. J., 1986. Adaptive management of renewable resources. Macmillan Publishers Ltd.
- 383 Weinstein, B. G., 2018. A computer vision for animal ecology. *Journal of Animal Ecology* 87 (3), 533–545.
- 384 Wilcove, D. S., Wikelski, M., 2008. Going, going, gone: is animal migration disappearing. *PLoS biology* 6 (7), e188.
- 385 Xue, Y., Wang, T., Skidmore, A. K., 2017. Automatic counting of large mammals from very high resolution panchromatic satellite imagery. *Remote*
386 *sensing* 9 (9), 878.
- 387 Yang, Z., Wang, T., Skidmore, A. K., de Leeuw, J., Said, M. Y., Freer, J., 2014. Spotting east african mammals in open savannah from space. *PLoS*
388 *one* 9 (12), e115989.